Aerodynamic Design Consideration for Stability of a Lightweight Solar-Powered Aircraft

Article *in* Path of Science · May 2022

DOI: 10.22178/pos.81-10

CITATIONS
2

READS
713

1 author:

Bashir Danjuma Safyanu
Abubakar Tatari Ali Polytechnic
10 PUBLICATIONS **31** CITATIONS

SEE PROFILE

Aerodynamic Design Consideration for Stability of a Lightweight Solar-Powered Aircraft

Safyanu Bashir Danjuma [1]

[1] *Abubakar Tatari Ali Polytechnic*
P. M. B. 0094, Bauchi, Bauchi State, Nigeria

DOI: 10.22178/pos.81-10

LCC Subject Category: L7-991

Received 16.04.2022
Accepted 28.05.2022
Published online 31.05.2022

Corresponding Author:
bashir.12393@yahoo.com

Abstract. Aerodynamic design analysis was conducted for the stability of a lightweight solar aircraft weighing 3 kg and a wingspan of 3.2 m. Airfoil analysis was conducted on four selected airfoils. The following factors were considered: good aerodynamic characteristics, low Reynolds number, high lift, low drag, high lift-to-drag ratio, quiet moment coefficient, moderate thickness, and camber curvature. WE-3.55.93 airfoil was selected as best and used to design the wing, and NACA 0008 was used to develop the empennage. The fuselage was designed with two compartments 1.9 m long, and the second compartment is made of aluminium or carbon fibre to reduce weight. The first compartment was 0.95 m long and 0.4 m in diameter. The centre of gravity was determined for the importance of the various aircraft components to ensure aerodynamic stability and balance. The complete assembly was designed using XFLR5 v6 software.

Keywords: aerodynamic design; airfoil analysis; high lift coefficient; low drag coefficient; centre of gravity.

INTRODUCTION

Solar aircraft, both manned and unmanned in today's world, have undergone dramatic improvements in aerodynamic stability, energy utilisation, energy conversion efficiency, and energy storage capability [7]. In addition, we have witnessed solar aircraft's ability to fly at a very high altitude and long endurance across the globe in a solar plane [3]. All of these are possible because of the technological advancement in solar aircraft aerodynamic stability and emerging technologies using lighter and stronger materials that can withstand the test of time [10, 15].

Global warming and natural disasters worldwide make fossil fuel use a significant threat because of their adverse effects on the environment [4]. The abundant solar energy availability is a great advantage to solar aircraft applications [16]. The mission feasibility is a path that guides the transition of a solar aircraft, when the solar energy is available from the climb to a higher altitude to the cruise stage during the day, to descend to a lower altitude, at night when the solar energy is not available [9].

Solar aircraft's challenges are the aerodynamic stability and capability to provide adequate space that accommodates the energy management system and the power device (Photovoltaic, rechargeable battery and maximum power point tracker) [15]. These components' lack of sufficient efficiencies makes solar aircraft performance low compared with fossil fuel aircraft [2]. The photovoltaic (PV) cell efficiency and energy density of solar aircraft's energy storage are too low to sustain a high altitude and long endurance flight. In contrast, conventional aircraft that use fossil fuel has a far higher energy density that can support long flight hours [1]. It's undeniable that a solar aircraft has a long way to go if it must compete with or replace conventional aircraft.

The study aims to conduct aerodynamic consideration for the stability of the lightweight solar aircraft with a weight of 3 kg and a wingspan of 3.2 m. Aerodynamic analysis of four airfoils was

conducted, and the best was selected and used for designing various parts of solar aircraft: wing, empennage, fuselage and complete assembly using XFLR5 v6. The aerodynamic considerations provide the necessary aerodynamic stability and accommodate the power device on the wings and in the fuselage of the solar aircraft.

METHODOLOGY

Airfoil Selection. Four airfoils were selected based on previous studies to develop an efficient and robust wing configuration, and an analysis was conducted to identify the most optimal among them using XFLR5 6v. The four airfoils are namely: AQUILA 9.3% [18], S9000 (9%) [11], S9037 (9%) [6] and WE-3.55 [12]. The airfoils were analysed under varying parameters from previous studies highlighted to validate and achieve optimal results: Reynold numbers (5.0×10^5–6.0×10^5) interval of 1.0×10^4 and angle of attack -3 °C to 15 °C, an increment of 1 °C. The following factors must be considered: good aerodynamic characteristics, low Reynolds number, high lift, low drag, high lift-to-drag ratio, quiet moment coefficient, moderate thickness, and camber curvature. According to [14], a 9 to 16 % thickness was most suitable for a home-built and solar-powered aircraft. NACA 0008 was selected as the most suitable airfoil; analysis was conducted and used for the empennage design [14].

Airfoil Analysis for Empennage Design. The solar aircraft design adopted convention-tail empennage; it is chosen to give room for more aerodynamic stability. Both the horizontal and vertical tail, symmetrical NACA 0008 four-digit airfoil, was used for the design. The airfoil has a thickness of 8 % and a panel number of 35. The tail airfoil often produces little lift compared to the wing airfoil.

Main Wing Design. Solar aircraft power output is meagre, contributing to the aircraft's difficulty in wing sizing compared to a conventional single-engine plane. The wing's surface area is subject to the amount of energy required from the solar radiation to power the aircraft and the total number of solar cells needed to produce the desired power. The wing configuration is adapted from similar aircraft with similar peculiarities in their mission specifications, as shown in Table 1. The adjusted mission parameters and aircraft shape variables are shown in Tables 2 and 3. The aircraft adopted a 7º polyhedral, tapered 0.2 m from the tip chord length of 0.5 m because it is more stable [18].

Table 1 – Aircraft Variables

Authors	Wingspan (m)	Chord (m)	Velocity (m/s)	Total Weight (kg)
[8]	3.3	0.28	-	3
[5]	3	0.25	-	3.46
[17]	6.28	0.9	10.93	24.96
[13]	3.2	0.25	8.3	2.6
[18]	2.63	0.28	7.5	2
[9]	4.25	0.32	-	5

Table 2 – Mission Parameters

Parameter	Units
Initial weight	3 kg
Payload	-
Airfoil chord	0.3 m
Altitude	1000 m
Average air density	1.1655 kg/m^3
Clearance factor	0.7 (1=clear sky)
Take–off distance	None (hand-tossed launch)

Table 3 – Aircraft Shape Variable

Parameter	Value	Unit
Aspect Ratio (AR)	11.25	
Wingspan (b)	3.2	m
The total weight (w)	3	kg

Empennage Design. The solar aircraft design adopted convention-tail empennage, giving room for more aerodynamic stability. Both the horizontal and vertical tail, symmetrical NACA 0008 four-digit airfoil, was used for the procedure. The tail airfoil often produces little lift compared to the wing airfoil. The Conventional-tail shape variables are shown in Table 4.

Table 4 – Conventional–Tail Shape Variable

Variable	Horizontal	Vertical
Tail span, m	0.7	0.3
Area, m^2	0.12	0.04
Aspect ratio	4.00	1.2
Taper ratio	1.33	1.00

Fuselage Design. The fuselage design of solar aircraft is quite different from conventional aircraft

because the load requirement is less, and no fuel or passenger is carried onboard. Instead, the fuselage components are the propeller's payload, autopilot computer, batteries, and motor. The sizing of the fuselage length, a relationship was adopted, a comparison of similar aircraft of the fuselage length with the wingspan [14].

$$\text{Fuselage length } F_L = b^{0.5289} \quad (1)$$

Centre of gravity and aircraft weight components. Stability analysis was conducted to determine the centre of gravity and aircraft weight components. The various design parts of the solar aircraft are designed and assembled using XFLR5 v6.

RESULTS AND DISCUSSION

Airfoil Analysis Results for Wing Design. Table 5 presents the results of four airfoils selected to develop an efficient and robust wing configuration.

The result shows that WE-3.55.93 was the best on the criteria set and was selected for the aircraft wing design. The aerodynamic characterisation and the four airfoils' comparisons were conducted on the direct foil analysis at 500,000 Reynolds number and 4° angles of attack, viewed at the operating point. The reason for choosing the particular Reynold number and the angle of attack is because the airfoils perform optimally at these points. However, the number of panels does not affect the aerodynamic behaviour of airfoils in this context.

Table 5 – The Aerodynamic Characterisation and Comparisons of the Airfoils

Airfoil	AQUILA-9.3%	S9000 (9%)	S9037 (9%)	WE-3.55
Thickness (%)	9.3	9.01	9.00	9.30
Max Camber (%)	4.05	2.37	3.49	3.55
CL	0.833	0.757	0.828	0.913
CD	0.008	0.008	0.008	0.008
C_L/C_D	101.911	93.235	104.897	117.248
Cm	-0.066	-0.066	-0.076	-0.110
No of Panels	69	121	121	117

Figure 1 shows the airfoil analysis with subfigures 1A to 1F.

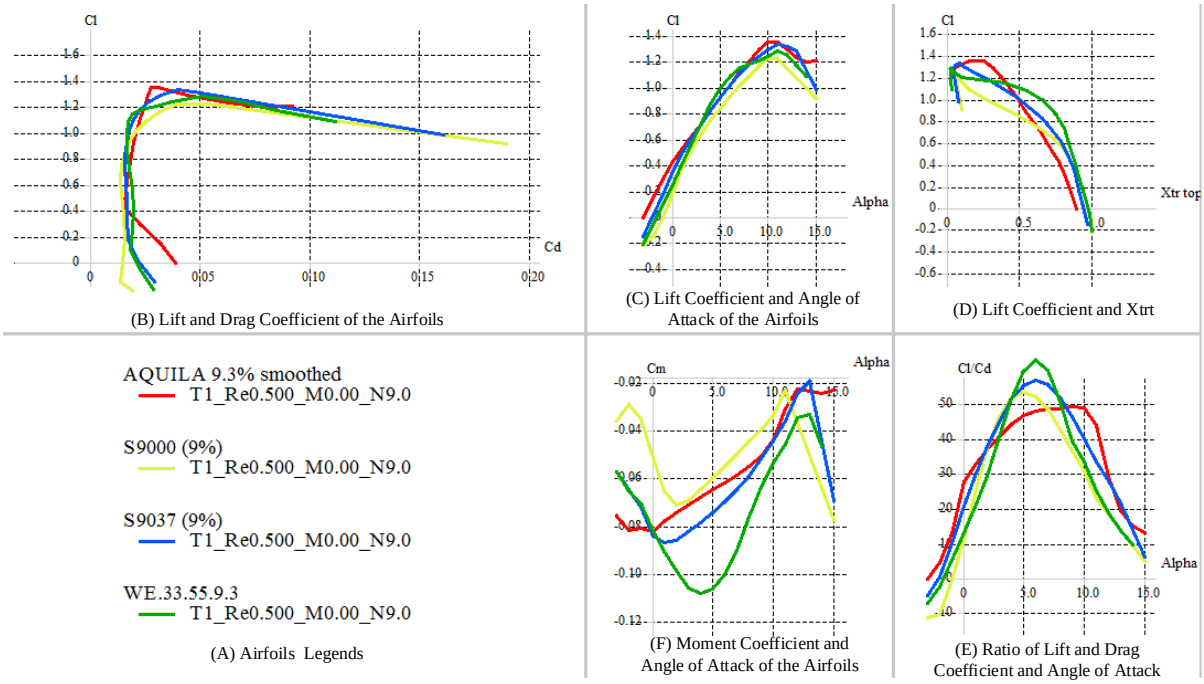

(B) Lift and Drag Coefficient of the Airfoils

(C) Lift Coefficient and Angle of Attack of the Airfoils

(D) Lift Coefficient and Xtrt

(A) Airfoils Legends

(F) Moment Coefficient and Angle of Attack of the Airfoils

(E) Ratio of Lift and Drag Coefficient and Angle of Attack

Figure 1 – Airfoil Analysis Polar View

Figure 1A is the legend with colours representing the airfoil types. Figure 1B depicts the drag coefficient's graph on the X-axis and lift coefficient on the Y-axis and their convergence on the opposing view. The chart shows all the airfoils have fully converged. Figure 1C presents the angle of attack

on the x-axis and the lift coefficient on the Y-axis. At 0 to 5 degrees, the WE.3.55 airfoil has the highest lift. Figure 1D shows the characterisation graph on the X-axis and the lift coefficient on the Y-axis. Also, all the airfoil converged. Figure 1E shows the X-axis's attack angle (alpha) and the Y-axis's lift/drag coefficient ratio. The graph shows that airfoil WE-3.55 has the highest lift/drag coefficient at 0 to 5 angles of attack. Figure 1F shows the moment coefficient and the angle of attack. It reveals that the WE-3.55 airfoil has a minor moment coefficient.

Airfoil Results for Empennage Design. A batch analysis was conducted on the selected airfoil NACA 0008 with Reynolds numbers ranging from 500,000 to 600,000 and the angle of attack going from -5 to 15 using XFLR5 v6 [18]. The operating points were viewed at 7 degrees angle of attack because the airfoil has the highest lift coefficient of 0.727, the highest lift/drag coefficient of 43.988, and a minor drag coefficient of 0.017. The opposing view presents five subgraphs that reveal the aerodynamic characteristics of the airfoil. The results are shown in Figures 2A to 2E.

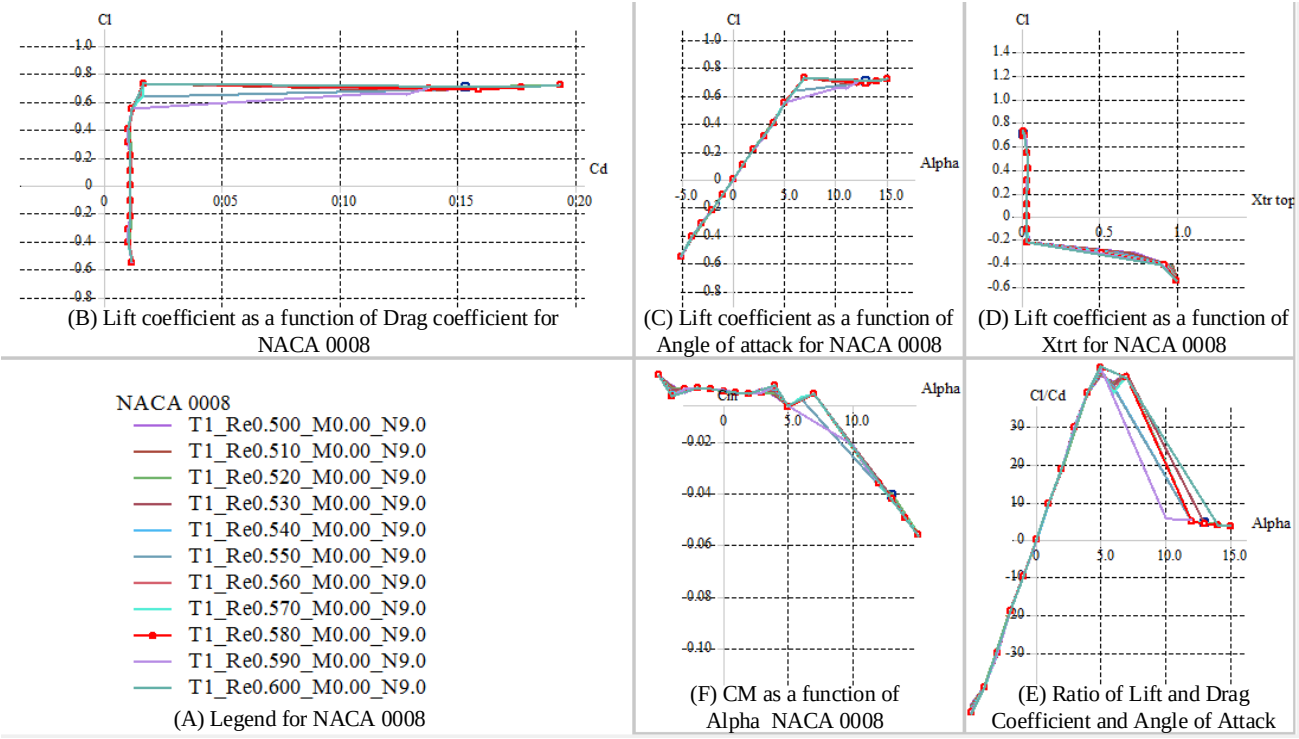

(B) Lift coefficient as a function of Drag coefficient for NACA 0008

(C) Lift coefficient as a function of Angle of attack for NACA 0008

(D) Lift coefficient as a function of Xtrt for NACA 0008

(A) Legend for NACA 0008

(F) CM as a function of Alpha NACA 0008

(E) Ratio of Lift and Drag Coefficient and Angle of Attack

Figure 2 – NACA 0008 Airfoil Analysis

Figure 2A depicts the legend representing the ranges of the Reynolds numbers in colours. Figure 2B captured the drag coefficient graph on the X-axis and the lift coefficient on the Y-axis. The Reynold number 580,000 has the most convergence on the chart and is highlighted with a red colour point curve line. Notwithstanding, other Reynold numbers show convergence. And all the graphs from Figures 2B to 2F show similar trends.

Results for the Main Wing Design. The aspect ratio and the wingspan in Table 4 were used to design the wing profile with the best-selected airfoil WE.3.55.9.3 using XFLR5 v6 software, as shown in Figure 3.

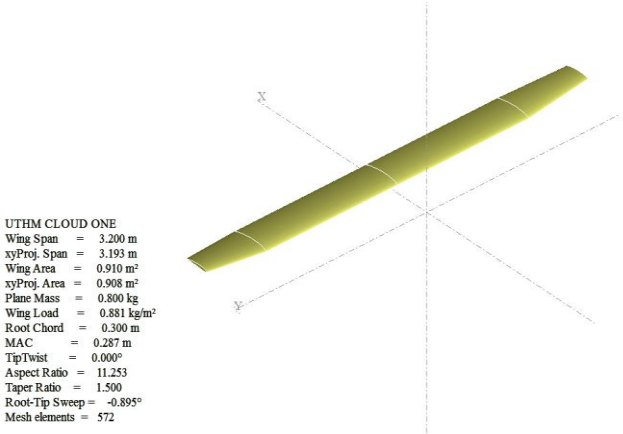

Figure 3 – Wing Design Profile using XFLR5 v6

Results for the Empennage Design. The horizontal tail (elevator) and vertical tail (fin) of the conven-

tional tail profile was designed with the adopted traditional configuration in Table 5 using XFLR5 v6 software, as shown in Figures 4 and 5.

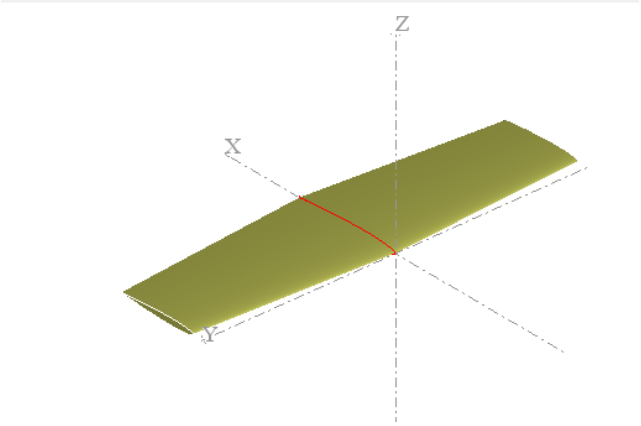

Figure 4 – Horizontal Tail

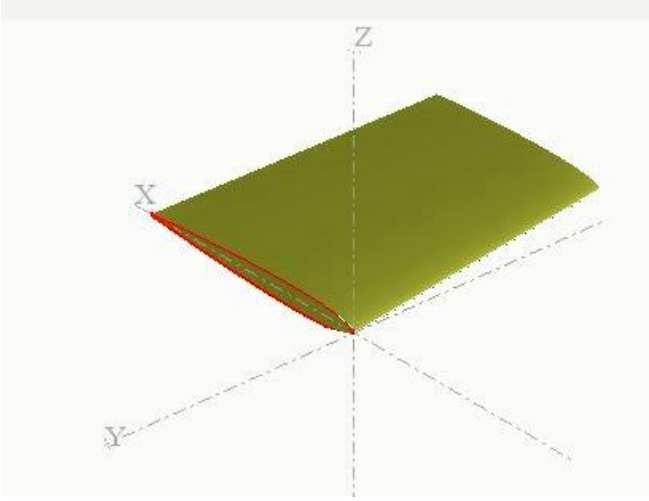

Figure 5 – Vertical tail

Results for the Fuselage Design. The fuselage length is found as 1.9 m by inputting the wingspan of 3.2 m in Equation 1. The fuselage design comprises two compartments. The first compartment is cylindrical and will house the payload, electronic, and propulsion equipment. The compartment's length covers from the tip to the midpoint of the fuselage length, 0.95 m. The diameter of the case was estimated to be around 0.4 m maximum to maintain aerodynamic stability [14]. At the same time, the second compartment of the fuselage is smaller and made of an aluminium tube or carbon fibre for simplicity and reduced weight. The fuselage design was conducted using XFLR5 v6 software, as shown in Figure 6.

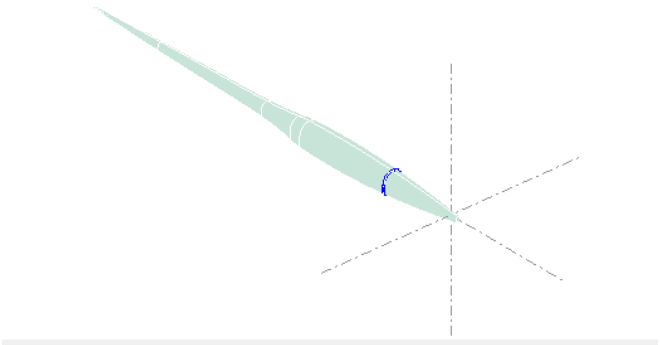

Figure 6 – Fuselage design profile

Results for the centre of gravity and aircraft weight components. Table 6 presents the centre of gravity and aircraft weight components.

Table 6 – Center of Gravity and Aircraft weight Components

Components	Weight, kg	Centre of Gravity		
		X_CoG, m	Y_CoG	Z_CoG
Wing	0.850	0.401	-0.000	0.063 m
Elevator	0.40	1.684	0.000	8.791×10^{-8}
Fin	0.20	1.714	1.124×10^{-7}	0.139
Fuselage	1.309	0.718	0.000	1.075×10^{-4}

The weights of the various aircraft components and their corresponding centre of gravity depict the aerodynamic stability and balance of the aircraft. Hence the multiple parts of the solar aircraft are designed and assembled using XFLR5 v6 software. The whole assembly in 3D views is shown in Figure 7.

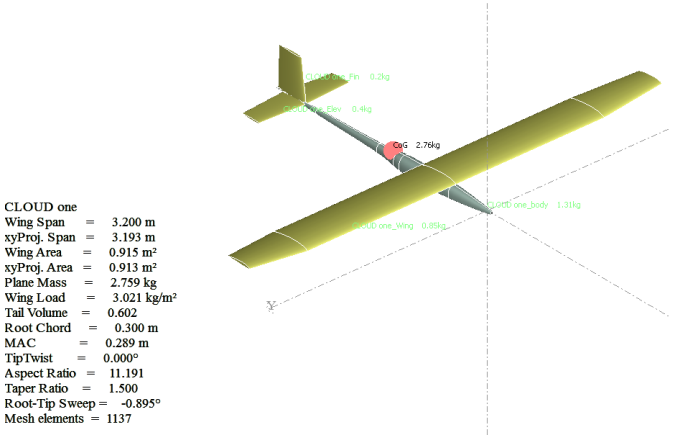

Figure 7 – 3D Full Assembly of the Solar-Powered Aircraft

CONCLUSIONS

Airfoil analysis was conducted for four selected airfoils. The best-performed airfoil in terms of the lowest drag coefficient, highest lift coefficient, and the lift-to-drag ratio, WE.3-55.93, was the best airfoil selected for the design. And NACA 0008 airfoil is the most suitable. Airfoil analysis was carried out and was used for the empennage design. The fuselage was designed, and the length was found as 1.9 m long. The fuselage is made of two-compartment. The first compartment covered 0.95 m from tip to midpoint with a 0.4 m diameter. The case is used to house the payload, electronics and propulsion equipment. The second compartment is made of carbon fibre or aluminium tube to reduce weight. The centre of gravity and weight of the various components of the aircraft were determined to ensure aerodynamic stability and balance of the plane. The whole assembly of the aircraft was done using XFLR5 v6 software.

REFERENCES

1. Abbe, G., & Smith, H. (2016). Technological development trends in Solar-powered Aircraft Systems. *Renewable and Sustainable Energy Reviews, 60*, 770–783. doi: 10.1016/j.rser.2016.01.053
2. Danjuma, S. B., Omar, Z., & Abdullahi, M. N. (2021). Design of Power Device Sizing and Integration for Solar-Powered Aircraft Application. *Journal of Mechanical Engineering, 18*(3), 215–232.
3. Davey, P. (2009, June 8-12). *Zephyr HALE UAS (High Altitude Long Endurance Unmanned Aerial System)*. Retrieved from https://apps.dtic.mil/sti/pdfs/ADA510880.pdf
4. Gao, X.-Z., Hou, Z.-X., Guo, Z., & Chen, X.-Q. (2015). Reviews of methods to extract and store energy for solar-powered aircraft. *Renewable and Sustainable Energy Reviews, 44*, 96–108. doi: 10.1016/j.rser.2014.11.025
5. Hargreaves, Z., Kim, B., Ou, A., Nguyen, Q., & Maharbiz, M. (2011, November 6). *Berkeley Solar Drone*. Retrieved from https://www.ocf.berkeley.edu/~qmn/lbl/resources/application/application-latex.pdf
6. Hartney, C. J. (2011). *Design of Small Solar-Powered Unmanned Aerial Vehicle* (Master's thesis). San Jose State University.
7. Hutchinson, H. (2016, October 7). Solar Impulse Closes the Circle. Retrieved from https://www.asme.org/topics-resources/content/solar-impulse-closes-the-circle
8. Khurana, A., Nayak, A., Pacholi, A., & Shah, R. (2014). *Design and Fabrications of Solar Powered Unmanned Aerial Vehicle*. Piani: IIT Bombay and Birla Institute of Technology and Science
9. Montgomery, S., & Mourtos, N. (2013). Design of a 5 Kilogram Solar-Powered Unmanned Airplane for Perpetual Solar Endurance Flight. *49th AIAA/ASME/SAE/ASEE Joint Propulsion Conference*. doi: 10.2514/6.2013-3875
10. Morton, S., D'Sa, R., & Papanikolopoulos, N. (2015). Solar powered UAV: Design and experiments. *2015 IEEE/RSJ International Conference on Intelligent Robots and Systems (IROS)*. doi: 10.1109/iros.2015.7353711
11. Najafi, Y. (2011). *Design of a High Altitude Long Endurance Solar Powered UAV SPACOM (Solar Powered Aerial Communicator)* (Master's thesis). San Jose State University.
12. Noth, A. (2008). *Design of Solar Powered Airplanes for Continuous Flight*. Retrieved from https://ethz.ch/content/dam/ethz/special-interest/mavt/robotics-n-intelligent-systems/asl-dam/documents/phd_thesis/Andre_Noth_Design_of_Solar_Powered_Airplanes_for_Continuous_Flight.pdf
13. Noth, A., & Siegwart, R (2008). *Design of Solar Powered Airplanes for Continuous Flight*. Retrieved from https://ethz.ch/content/dam/ethz/special-interest/mavt/robotics-n-intelligent-systems/asl-dam/documents/projects/Design_Skysailor.pdf

14. Raymer, D. P. (2007). *Simplified Aircraft Design for Home Builders*. Los Angeles: Design Dimension Press.

15. Safyanu, B. D., Abdullah, M. N., & Omar, Z. (2019). Review of Power Device for Solar-Powered Aircraft Applications. *Journal of Aerospace Technology and Management, 11*. doi: 10.5028/jatm.v11.1077

16. Safyanu, B. D., Omar, Z., & Abdullahi, M. N. (2018). Review of Photovoltaic Cells for Solar-Powered Aircraft Applications. *International Journal of Engineering & Technology, 7*, 131–135.

17. Shiau, J.-K., Ma, D.-M., Chiu, C.-W., & Shie, J.-R. (2010). Optimal Sizing and Cruise Speed Determination for a Solar-Powered Airplane. *Journal of Aircraft, 47*(2), 622–629. doi: 10.2514/1.45908

18. Sri, K. R. B., Aneesh, P., Bhanu, K., & Natarajan, M. (2016). Design Analysis of Solar-Powered Unmanned Aerial Vehicle. *Journal of Aerospace Technology and Management, 8*(4), 397–407. doi: 10.5028/jatm.v8i4.666